

# Subthreshold behavior and avalanches in an exactly solvable Charge Density Wave system

David C. Kaspar<sup>1</sup> and Muhittin Mungan<sup>2</sup>

<sup>1</sup> *Mathematics Department, University of California, Berkeley, CA 94720, USA, and*

<sup>2</sup> *Physics Department, Boğaziçi University, Bebek 34342 Istanbul, Turkey*

(Dated: June 26, 2018)

We present a toy charge density wave (CDW) model in 1d exhibiting a depinning transition with threshold force and configurations that are explicit. Due to the periodic boundary conditions imposed, the threshold configuration has a set of topological defects whose location and number depend on the realization of the random phases. Approaching threshold, these defects are relocated by avalanches whose size dependence on the external driving force  $F$  is described by a record-breaking process. We find that the depinning transition in this model is a critical phenomenon, with the cumulative avalanche size diverging near threshold as  $(F_{\text{th}} - F)^{-2}$ . The exact avalanche size distributions and their dependence on the control parameter  $(F_{\text{th}} - F)$  are obtained. Remarkably, the scaling exponents associated with the critical behavior depend on (1) the initial conditions and (2) the relationship between the system size and the pinning strength.

PACS numbers: 05.40.-a,64.60.Ht,45.70.Ht

The motion of Charge Density Waves (CDW) belongs to the class of systems in which an elastic structure is driven by external forces through a random medium. Fisher [1, 2] has argued that the depinning transition, when the deformable medium begins to slide, is a *dynamic critical phenomenon*: a phase transition with the driving force as the control parameter. Analytical results for the divergence of strains [3, 4], functional renormalization group calculations [5–7], and extensive numerical simulation of CDW and similar systems in dimensions  $d = 1, 2, 3$  [8–14] support this claim. However, there are few *rigorous* results providing evidence whether the depinning transition is indeed a critical phenomenon, particularly in  $d = 1$ . In this letter we introduce an exactly solvable CDW model in  $d = 1$  that exhibits the tell-tales of a critical phenomenon and allows us to understand the origin of criticality.

We begin with the CDW Hamiltonian and some accompanying notation. Let

$$\mathcal{H}(\{y_i\}) = \sum_i \frac{1}{2}(y_i - y_{i-1})^2 + V(y_i - \alpha_i) - Fy_i, \quad (1)$$

where  $V(x)$  is 1-periodic and  $\alpha_i$ , the impurity phases, are *i.i.d.* uniform on  $(-\frac{1}{2}, +\frac{1}{2})$ . Following Narayan and Fisher [5], we choose

$$V(x) = \frac{\lambda}{2}(x - \llbracket x \rrbracket)^2. \quad (2)$$

Here  $\lambda$  is the strength of the potential and  $\llbracket x \rrbracket$  is the nearest integer to  $x$ . Write

$$m_i \equiv \llbracket y_i - \alpha_i \rrbracket \quad \text{and} \quad \tilde{y}_i \equiv y_i - \alpha_i - m_i, \quad (3)$$

for the *well number* and *well coordinate* of  $y_i$ ; the former records which parabolic well contains  $y_i$  and the latter the displacement in  $(-\frac{1}{2}, +\frac{1}{2}]$  from the well's center.

For static configurations the piecewise-parabolic potential permits an explicit formula for  $\tilde{y}_i$  in terms of the

well numbers  $m_i$  and the phases  $\alpha_i$ ,

$$\tilde{y}_i = \frac{\eta}{1 - \eta^2} \sum_{j \in \mathbb{Z}} \eta^{|i-j|} (\Delta \alpha_j + \Delta m_j) + F/\lambda. \quad (4)$$

Here  $\Delta$  is the discrete Laplace operator,  $\Delta \alpha_i = \alpha_{i-1} - 2\alpha_i + \alpha_{i+1}$ , and  $0 < \eta < 1$  is the smaller root of  $\eta^2 - (2 + \lambda)\eta + 1 = 0$ . The nonlinearity of the system is an admissibility condition:  $m_i$  must be such that (4) gives  $\tilde{y}_i \in (-\frac{1}{2}, +\frac{1}{2}]$ . One can check that all static configurations are linearly stable unless a particle is at a cusp of  $V$ . We investigate the case where  $m_i$  and  $\alpha_i$  are  $L$ -periodic, the latter still *i.i.d.* within a single period.

Consider the behavior of this system starting from some initial configuration and increasing the force. We assume that the dynamics of the particles are purely relaxational and that all changes in the force are sufficiently slow that we reach the static configurations. From (4) it follows that increasing  $F$  translates all particles uniformly until the first particle, say  $j$ , reaches a cusp,  $\tilde{y}_j = 1/2$ . Any further infinitesimal increase causes particle  $j$  to jump wells  $m_j \rightarrow m_j + 1$ , displacing

$$\tilde{y}_k \rightarrow \tilde{y}_k - \delta_{jk} + \frac{1 - \eta}{1 + \eta} \eta^{|j-k|}, \quad (5)$$

which may cause other particles to cross  $+\frac{1}{2}$  and jump as well, and so on. Depending on  $F$  this process may terminate, yielding another stable configuration, or continue forever, which we interpret as the sliding state.

Like the CDW models with sinusoidal potential [13, 14], this model exhibits behavior which is:

- *Irreversible*. If we change the force by  $\Delta F$ , causing one or more particles to jump wells before reaching another stable configuration, and then return  $F$  to its original value, *none* of the particles jump back [15].

- *Reversible.* The resulting configuration reacts by rigid translation, without jumps, to forces in the interval between  $F$  and  $F + \Delta F$ .

To focus on the irreversible dynamics, we identify configurations at nonzero  $F$  with their  $F = 0$  versions (*zero-force configurations*) which have the same well numbers  $m_i$ , provided that the well coordinates  $\tilde{y}_i$  of the latter react to  $F$  by rigid translation only.

## I. THE TOY MODEL

We simplify our CDW model further by choosing  $\lambda$  large ( $\eta$  small): defining rescaled well coordinates  $z_i$  by  $\eta z_i = \tilde{y}_i - F/\lambda$ , we obtain from (4)

$$z_i = \Delta\alpha_i + \Delta m_i + O(\eta). \quad (6)$$

We will refer to the CDW model, dropping  $O(\eta^2)$  terms ( $O(\eta)$  after rescaling), as the *toy model*; here we have nearest-neighbor interactions only and obtain a set of exact results. Proofs and additional results for the untruncated model will be given elsewhere [15].

For the toy model, the process of increasing the external force and evolving the configurations to threshold can be described by the following *zero-force algorithm* (ZFA), which operates on  $L$ -periodic zero-force configurations:

(ZFA1) Record  $z_{\max} = \max_i z_i$ .

(ZFA2) Find  $j = \arg \max_i z_i$  and set

$$\begin{aligned} m_j &\rightarrow m_j + 1 \\ z_{j\pm 1} &\rightarrow z_{j\pm 1} + 1 \\ z_j &\rightarrow z_j - 2. \end{aligned} \quad (7)$$

(ZFA3) If any  $z_i > z_{\max}$  from (ZFA1), goto (ZFA2).

The initial execution of (ZFA2) jumps the particle which would first reach the cusp *if* the force were increased, and subsequent executions (if any) resolve those particles which would be pulled across the cusp as a result of the first. We note the following properties of the ZFA:

- (i) The ZFA always terminates, with all sites having jumped at most once.
- (ii) If in secondary executions of (ZFA2) we take  $j$  to be any site where  $z_j > z_{\max}$ , not necessarily the maximum, the final result is unchanged.
- (iii) If all sites jump, then the  $z_i$  are unchanged, and this fixed-point is the threshold configuration.
- (iv) The ZFA finds the threshold configuration after a number of iterations which is bounded by a function of the system size  $L$ .

As noted for similar CDW models [10, 14, 16], (ZFA2) suggests a connection to Abelian sandpile models; see Redig [17] for an introduction. In that setting, the change (7) in  $z$  would be called *toppling* at  $j$ , and (ii) above is precisely the Abelian property. Note, however, that although a variety of sandpile models with slightly varying features have been studied previously (see [18] for a survey and [19] for a model which also has continuous heights), what we call the toy model does not seem to be among them. Our model has periodic boundary; is conservative in that  $z$  “mass” is moved about, but neither added nor removed; evolves deterministically, with integer changes only; and has a random fractional part from the initial conditions which is preserved by the dynamics.

## II. THRESHOLD CONFIGURATIONS

The ZFA indicates that the evolution to the depinning transition under force increments minimizes  $\max_i z_i$ , and indeed the threshold configuration is the solution of the variational problem [20]  $\min_m \max_i z_i$ . From this perspective (6) suggests  $\Delta m_i = -\llbracket \Delta\alpha_i \rrbracket$  would be favorable, but periodicity and the requirement that  $m_i \in \mathbb{Z}$  usually prevent this. We need only choose to deviate from this guess in the most favorable places.

Let  $S \equiv \sum_{i=0}^{L-1} \llbracket \Delta\alpha_i \rrbracket$ . The threshold configuration  $\{m_i^+\}$  satisfies

$$\Delta m_i^+ = -\llbracket \Delta\alpha_i \rrbracket + J_i^+ - \delta_{ik^+} \quad (8)$$

where  $J$  is an integer vector selected as follows:

- (i) *Case  $S \geq 0$ .*  $J_i^+ = 1$  for the  $S + 1$  positions  $i$  which have smallest  $\Delta\alpha_i - \llbracket \Delta\alpha_i \rrbracket$ ,  $J_i^+ = 0$  otherwise;
- (ii) *Case  $S < 0$ .*  $J_i^+ = -1$  for the  $|S| - 1$  positions  $i$  which have largest  $\Delta\alpha_i - \llbracket \Delta\alpha_i \rrbracket$ ,  $J_i^+ = 0$  otherwise;

and  $k^+$  is an index defined by (*divisibility condition*)

$$k^+ \equiv \sum_{i=0}^{L-1} i(-\llbracket \Delta\alpha_i \rrbracket + J_i^+) \pmod{L}. \quad (9)$$

The proof is straightforward and given in [15]. We will refer to those sites where  $\Delta m_i^+ + \llbracket \Delta\alpha_i \rrbracket \equiv \epsilon_i \neq 0$  as *defects* with *charge*  $\epsilon_i$ .

## III. THE DEPINNING THRESHOLD FORCE

Using (8), the threshold configuration  $z_i^+$  for the toy model is explicit, as is the threshold force:

$$F_{\text{th}}(\{\alpha_i\}) = \lambda(1/2 - \eta z_{\max}^+), \quad (10)$$

where  $z_{\max}^+ \equiv \max_i z_i^+$ . The term in parentheses on the right-hand side is the distance from the particle with maximum  $z_i$  to the cusp. Defining

$$\omega_i \equiv \Delta\alpha_i - \llbracket \Delta\alpha_i \rrbracket \quad (11)$$

and using (6) and (8), we find that[21]

$$z_{\max}^+ = \begin{cases} \omega_{\sigma(S)} + 1 & \text{if } S \geq 0 \\ \omega_{\sigma(L-|S|)} & \text{if } S < 0 \end{cases} \quad (12)$$

where  $\sigma$  is the permutation of the indices that orders  $\omega$ :

$$\omega_{\sigma(0)} < \omega_{\sigma(1)} < \cdots < \omega_{\sigma(L-1)}.$$

We therefore understand the dependence of  $z_{\max}^+$  on the random phases  $\alpha_i$  as coming almost exclusively from the sum  $S = -\sum_{i=0}^{L-1} \omega_i$  and rank statistics of  $\{\omega_i\}$ .

It turns out [15] that any  $L-1$  (but not all  $L$ ) of the  $\omega_i$  are *i.i.d.* uniform  $(-\frac{1}{2}, +\frac{1}{2})$ , whence routine arguments show  $L^{-1/2}S$  converges in distribution as  $L \rightarrow \infty$  to a normal random variable with mean 0 and variance 1/12. Thus the typical number of topological defects scales as  $L^{1/2}$ , and the threshold force averaged over the quenched disorder is found to be

$$\mathbb{E}F_{\text{th}} = (1 - \eta)^3/2\eta + O(L^{-3/2}). \quad (13)$$

The variance  $(\Delta F_{\text{th}})^2$  scales as

$$(\Delta F_{\text{th}})^2 \sim L^{-1}. \quad (14)$$

so that fluctuations  $\Delta F_{\text{th}}$  scale as  $L^{-1/2}$ . This matches the scaling behavior of the sinusoidal CDW model [13, 14], for which the expected behavior is  $\Delta F_{\text{th}} \sim L^{-1/\nu_{FS}}$ , with  $\nu_{FS}$  the finite-size scaling exponent from the scaling theory of Chayes *et al* [22]. Our model saturates their prediction  $\nu_{FS} \geq 2/d$  in  $d = 1$  with

$$\nu_{FS} = 2. \quad (15)$$

#### IV. FLAT IC TO THRESHOLD

We are interested not only in the threshold state itself, but also the changes that occur as we drive the system toward it. One might start with any stable configuration, but two initial conditions seem particularly natural. Here we treat the ‘‘flat’’ case,  $m_i = 0$  for all  $i$ , and address the other in the next section.

The primary quantity of interest is the *cumulative avalanche size*  $\Sigma$ , *i.e.* the total number of jumps which occur, or equivalently the *polarization*  $P = \Sigma/L$ . For the flat IC,

$$\Sigma = \sum_{i=0}^{L-1} m_i^+ \quad (16)$$

where  $\{m_i^+\}$  are the well numbers of the unique threshold configuration with  $\min_i m_i^+ = 0$ . The characterization (8) can be used to obtain the scaling behavior of  $\Sigma$  and  $P$  with  $L$ .

The key observation is that components of  $\{z_i^+\}$  are *exchangeable*, *i.e.* their joint distribution is invariant under permutations [15]. This leads directly to a scaling

limit for the threshold *strains*  $s_i \equiv m_i^+ - m_{i-1}^+$ . Define a *rescaled strain process*  $s^{(L)}(t)$  by

$$s^{(L)}(t) \equiv (L/12)^{-1/2} s_{\lfloor Lt \rfloor} \quad (0 \leq t \leq 1). \quad (17)$$

These processes in the *Skorokhod space*[23]  $\mathcal{D}([0, 1])$  converge in distribution to a Brownian bridge with zero integral [15]. More precisely, the limiting distribution is that of

$$B(t) - \int_0^1 B(r) dr \quad (18)$$

where  $B(t)$  is the Brownian bridge, the result of conditioning Brownian motion to return to 0 at  $t = 1$ .

This implies that the typical maximum and minimum of  $(s_i)$  at threshold is diverging like  $L^{1/2}$ , as expected from the work of Coppersmith [3, 4], but also more: as  $(s_i)$  is the discrete derivative of  $(m_i^+)$ , we integrate it twice [15] to find that

$$\Sigma \sim L^{5/2} \quad \text{and thus} \quad P \sim L^{3/2} \quad (19)$$

for typical realizations of the randomness.

#### V. THRESHOLD TO THRESHOLD

Taking the *negative* threshold configuration as our initial condition [13, 14], we can give a more complete picture, including the beginning, the end, and also the intermediate states observed as we iterate the ZFA.

We first adapt (8) for the negative threshold configuration, which maximizes  $\min_i z_i$ . Define  $J^-$  and  $k^-$ :

- (i) *Case*  $S > 0$ .  $J_i^- = 1$  for the  $S-1$  positions  $i$  which have smallest  $\omega_i$ ,  $J_i^- = 0$  otherwise;
- (ii) *Case*  $S \leq 0$ .  $J_i^- = -1$  for the  $|S|+1$  positions  $i$  which have largest  $\omega_i$ ,  $J_i^- = 0$  otherwise;

and  $k^-$  is given in terms of  $J^-$  by analogy with (9).

It is convenient to introduce

$$\zeta_i = \omega_i + J_i^- \quad (20)$$

and the permutation  $\pi$  that orders  $\zeta$ :

$$\zeta_{\pi(0)} < \zeta_{\pi(1)} < \cdots < \zeta_{\pi(L-1)}. \quad (21)$$

Note  $\zeta_{\pi(L-1)} - \zeta_{\pi(0)} < 1$ . The  $(\pm)$ -threshold configurations have

$$z_i^- = \zeta_i + \delta_{ik^-} \quad (22)$$

$$z_i^+ = \zeta_i + \delta_{i\pi(0)} + \delta_{i\pi(1)} - \delta_{ik^+}, \quad (23)$$

and, using the divisibility condition,  $k^\pm$  are related by[24]

$$k^+ = \pi(0) + \pi(1) - k^-. \quad (24)$$

Applying the ZFA to the negative threshold configuration,  $z_{\max} = \zeta_{k^-} + 1$  and  $k^-$  is the first site to jump:

$$\begin{aligned} z_{k^-} &= \zeta_{k^-} + 1 & \rightarrow & & z_{k^-} &= \zeta_{k^-} - 1 \\ z_{k^- \pm 1} &= \zeta_{k^- \pm 1} & \rightarrow & & z_{k^- \pm 1} &= \zeta_{k^- \pm 1} + 1. \end{aligned}$$

The neighboring sites  $k^- \pm 1$  will be forced to jump if  $\zeta_{k^- \pm 1} > \zeta_{k^-}$ ; this process continues for all those *consecutive* neighbors  $i$  to the left and right of  $k^-$  for which  $\zeta_i > \zeta_{k^-}$ . Write  $i_L$  and  $i_R$  for the first sites on the left and right, respectively, of  $k^-$  which have

$$\zeta_{i_L}, \zeta_{i_R} \leq \zeta_{k^-} \quad (25)$$

and thus will *not* be forced to jump.

If jumps occur at both sites  $k^- \pm 1$ , then  $z_{k^-}$  is unchanged, hence still the maximum, and the next ZFA also begins at  $k^-$ . This observation allows us to identify the *avalanche* consisting of all consecutive ZFA iterations initiated at a common site; the individual iterations which constitute it will be called *avalanche waves* [25]. Given an initial site  $i$ , with sites  $i_L$  and  $i_R$  — the closest on the left and right which do not jump in the first avalanche wave — the avalanche finishes after  $\min(i - i_L, i_R - i)$  waves with a total of  $(i - i_L)(i_R - i)$  jumps [15].

To better understand the threshold-to-threshold evolution under the ZFA, observe that the ranks  $\pi(j)$  of the  $\zeta_j$  suffice to determine the avalanche's initial site and extents. We represent a given configuration  $z_j$  by displaying the rank  $\pi(j)$  of  $\zeta_j$  and using over- or underlines to indicate additions by  $\pm 1$  which are acquired as a result of jumps:

$$\overline{\pi(j)} \leftrightarrow z_{\pi(j)} = \zeta_{\pi(j)} + 1, \quad (26)$$

$$\underline{\pi(j)} \leftrightarrow z_{\pi(j)} = \zeta_{\pi(j)} - 1. \quad (27)$$

For example, suppose that  $z^-$  has the rank representation

$$\dots 0 \ 10 \ 12 \ 17 \ \overline{15} \ 16 \ 18 \ 11 \ 13 \ 1 \ \dots$$

so that  $\pi(k^-) = 15$ . The extents of the first avalanche wave are  $k^- - i_L = 2, i_R - k^- = 3$  and after the sites bracketed below have jumped, the resulting configuration is

$$\dots 0 \ 10 \ \overline{12} \ \underline{17} \ \overline{15} \ 16 \ \underline{18} \ \overline{11} \ 13 \ 1 \ \dots$$

In the second wave,  $k^-$  and  $k^- + 1$  jump again, yielding

$$\dots 0 \ 10 \ \overline{12} \ 17 \ \underline{15} \ \underline{16} \ 18 \ \overline{11} \ 13 \ 1 \ \dots,$$

and the avalanche is complete. The remaining avalanches begin at the sites ranked 12, 11, and 10; the result is the positive threshold configuration.

This example illustrates that the important sites in the threshold-to-threshold evolution are the *lower records* [26, 27]: given a sequence of values  $X_1, X_2, \dots$ , we say that  $X_i$  is a *lower record* if  $X_i = \min\{X_j : j \leq i\}$ . Using (25)

we see that avalanches are determined by the locations of the lower records of the sequences

$$\mathcal{J}_L = \zeta_{k^-}, \zeta_{k^- - 1}, \zeta_{k^- - 2}, \dots, \zeta_{\pi_L}, \quad (28)$$

$$\text{and } \mathcal{J}_R = \zeta_{k^-}, \zeta_{k^- + 1}, \zeta_{k^- + 2}, \dots, \zeta_{\pi_R}, \quad (29)$$

where  $\{\pi_L, \pi_R\} = \{\pi(0), \pi(1)\}$  are the termination sites. The evolution from negative to positive threshold terminates when the avalanches reach  $\pi_L$  and  $\pi_R$ .

For use in the next section we note the following [15]:

- The variates  $\zeta_i$  are exchangeable.
- Thus  $\pi_L$  and  $\pi_R$  are selected uniformly from all pairs of (distinct) indices.
- In fact,  $k^-$  is independent of  $\pi$ .

## VI. AVALANCHE SIZE DISTRIBUTIONS

We are interested in the cumulative avalanche size  $\Sigma$  and obtain in this section a parametric family of distributions in the  $L \rightarrow \infty$  limit.

As we move from  $(-)$ -threshold to  $(+)$ -threshold, let  $X = z_{\max} - z_{\max}^+$  be the current maximum height minus that of the  $(+)$ -threshold configuration;  $X \in [0, 1)$ . Shift indices so that  $k^- = 0$ , and let  $j_L(x)$  and  $j_R(x)$  be the noninclusive left and right endpoints of the interval of sites that have jumped in the threshold-to-threshold evolution to achieve  $X \leq x$ , chosen so that  $-L < j_L \leq 0 \leq j_R < j_L + L$ . Observe that  $j_L$  and  $j_R$  take values which are indices of lower records: in fact,  $j_L(x)$  and  $j_R(x)$  are the first indices in  $\mathcal{J}_L$  and  $\mathcal{J}_R$  for which  $\zeta_i \leq \zeta_{\pi(1)} + x$ .

If  $\{m_i(x)\}$  are the well numbers of the first configuration with  $X \leq x$ , the corresponding avalanche size is

$$\Sigma(x) = \sum_{i=0}^{L-1} (m_i(x) - m_i^-) = |j_L(x)| j_R(x). \quad (30)$$

The simplicity of (30) is due to the geometry of  $\{m_i(x) - m_i^-\}$  in the threshold-to-threshold case, which deviates from 0 in only a single (discrete) trapezoidal bump [15]. Through (30) we address the statistics of  $\Sigma(x)$ .

For large  $L$ , approximate  $\zeta_{\sigma(1)} = -\frac{1}{2}$  and  $\zeta$  in  $\mathcal{J}_L$  and  $\mathcal{J}_R$  as *i.i.d.* uniform  $(-\frac{1}{2}, +\frac{1}{2})$  variates, sharing their first elements. Then  $j_L$  and  $j_R$  are truncated [28] geometric random variables. Setting  $u = Lx$ , one shows that as  $L \rightarrow \infty$  the distribution of the pair

$$\left( \frac{|j_L(u/L)|}{L}, \frac{j_R(u/L)}{L} \right) \quad (31)$$

converges to a truncation of a pair of exponential random variables with rate  $u$ . One then obtains for each value of  $u$  the limiting probability density of the rescaled avalanche size,  $\varsigma(u) \equiv \lim_{L \rightarrow \infty} \Sigma(u/L)/L^2$  [15]:

$$p_u(s) = \int_{2\sqrt{s}}^1 dz e^{-zu} \frac{4 + 8u(1-z) + 2u^2(1-z)^2}{(z^2 - 4s)^{1/2}}, \quad (32)$$

which is supported on  $[0, \frac{1}{4}]$ . In particular, when  $u = 0$ , we obtain the distribution of the rescaled total number of jumps  $\zeta(0)$  in the threshold-to-threshold evolution,

$$p_0(s) = 2 \ln \frac{1 + \sqrt{1 - 4s}}{1 - \sqrt{1 - 4s}}. \quad (33)$$

Note that (33) is precisely the avalanche size distribution of Dhar's Abelian sandpile model in  $d = 1$  considered by Ruelle and Sen [17, 29–31]. This connection is not an accident [15]: the total threshold-to-threshold evolution, without intermediate details, maps to a recurrent sandpile configuration, a site at which sand is added, and the resulting toppling. However, this map loses information, specifically the ordering and values of the well coordinates  $z_i$ , which are necessary to obtain the complete family (32).

From (32) we find the rescaled mean avalanche size,  $\lim_{L \rightarrow \infty} L^{-2} \mathbb{E}[\Sigma(u/L)] \equiv \Phi(u)$ , as

$$\Phi(u) = \frac{6 - 4u + u^2 - 6e^{-u} - 2ue^{-u}}{u^4}. \quad (34)$$

For  $0 < u \ll 1$ , we find

$$\Phi(u) = 1/12 - u/30 + u^2/120 - u^3/105 + O(u^4) \quad (35)$$

while for  $u \gg 1$  we have  $\Phi(u) \sim u^{-2}$ , with a crossover near  $u = XL = 1$  (inset of Figure 1). The exponent of  $-2$  in the scaling regime is typically denoted by  $-\gamma + 1$  [2, 14], so that  $\gamma = 3$ .

The crossover and the scaling exponent can be motivated via record sequences. Given a current record  $X$ , the next record will occur on average after  $1/X$  sites. Since all sites within this range are forced to jump, this defines the correlation length  $\xi \sim X^{-\nu}$ , with exponent  $\nu = 1$ . The crossover to the saturated regime occurs when  $\xi$  is comparable to  $L$ , namely  $u = XL \sim L/\xi \sim 1$ . The size (30) of an avalanche depends on the product of its left and right extents and thus scales as  $X^{-2}$ .

In the scaling regime, corresponding to large values of  $u$ , an asymptotic expansion of  $p_u(s)$  in  $u$  shows that the distribution obtains a scaling form in terms of the variable  $a = u^2s$ ,

$$p(a) = 2K_0(2\sqrt{a}), \quad (36)$$

where  $K_0$  is the modified Bessel function, which decays at large values of its argument as  $e^{-2u\sqrt{s}}/(2u\sqrt{s})^{1/2}$ . For the  $u$ -values shown in Fig. 1, the asymptotic form (36) is indistinguishable from the exact result (32), explaining the collapse of the data. The form of the scaling variable  $a$  can be understood by noting that  $a = u^2s = X^2\Sigma = \Sigma/\xi^2$ ; thus the avalanche sizes are measured in units of  $\xi^2$ .

## VII. COMPARISON WITH THE FULL MODEL

The scaling exponents for the threshold-to-threshold evolution of the toy model ( $\nu = 1, \gamma = 3$ ) differ from

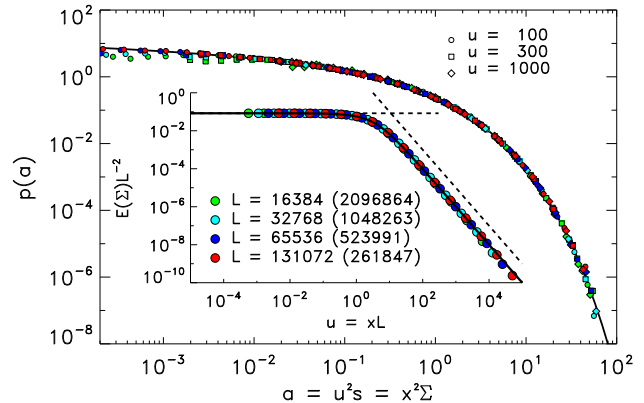


FIG. 1. Numerical cumulative avalanche size distribution for various  $L$  and  $u$ . For large  $u$ , the distributions collapse when avalanche sizes are scaled as  $a = u^2s$ . The solid line is (32). Inset: Finite-size scaling behavior of the mean cumulative avalanche size. The horizontal and slanted dashed line correspond to  $\Phi(0)$  in (35), and a power law of exponent  $-2$ , respectively. The solid line is the finite size scaling function (34). Symbol colors refer to different  $L$  as indicated in the legend, where the numbers of realizations are shown in parentheses.

those obtained via the  $4 - \epsilon$  expansion of Narayan *et al* [5, 14], ( $\nu = 2, \gamma = 4$ ) in 1d, but agree with those of the  $d = 1$  CDW automaton model of Myers and Sethna [10]. To investigate this discrepancy, we have simulated the full CDW model (4) at small values of  $\lambda$ . The results are shown in Fig. 2. Remarkably, our results suggest a crossover in the finite-size scaling behavior, from that of the toy model at small system sizes  $L$  to the prediction of Narayan *et al* at larger  $L$ . For  $\lambda = 10$  this crossover occurs around  $L_c = 500$ . Also,  $L_c$  increases with  $\lambda$ .

The presence of a  $\lambda$ -dependent length scale  $L_c$  might also explain why clean critical behavior in 1d CDW models was not seen in numerical simulations carried out in the 1990s [10, 13]: the feasible system sizes of those years were probably not large enough to push the simulations out of the crossover region, (*see* Figs. 5 and 18 in [13]).

We also performed numerical simulations of the toy model with flat initial condition and find scaling of the polarization that *does* match that of Narayan *et al* with  $\gamma = 4$  and  $\nu = 2$ , which is also consistent with our analytical result,  $P \sim L^{3/2}$  at threshold, (19).

## VIII. DISCUSSION

We have presented an exactly solvable CDW toy model in 1d with a critical depinning transition, exposing the roles played by the disorder and the boundary conditions. The evolution towards threshold is a process of breaking lower records on the coordinates of the particles in their unit cells. This is a direct consequence of the fact that as threshold is approached, larger segments are displaced and the increasing stress at their boundaries has to be re-

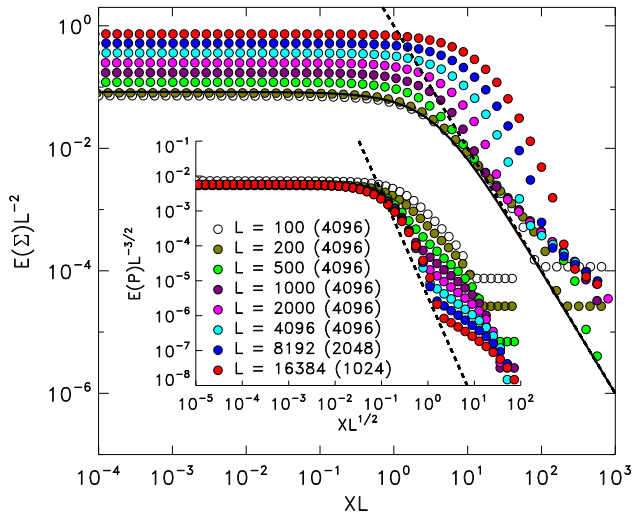


FIG. 2. Finite-size scaling behavior of CDW model for  $\lambda = 10$ . The system sizes and number of realizations are as indicated in the legend of the inset. Main figure: Finite-size scaling of the expected avalanche size at reduced force  $X$ , using the scaling of the toy model  $\gamma = 3$ ,  $\nu = 1$ . The solid line is the theoretical expression (22) obtained for the toy model, while the slanted dashed line indicates a power law with exponent  $-2$ . Inset: plot of the expected polarization  $P = \Sigma/L$  against  $X$  using the scaling predicted by Narayan *et al.*,  $\gamma = 4$ ,  $\nu = 2$ . The dashed line indicates a power law with exponent  $-3$ .

lied by particles which have sufficient room to advance without jumping.

Our numerical results for the scaling behavior of the full model (4) show a crossover from the finite-size scaling of the toy model for  $L < L_c$  to the scaling predicted by Narayan *et al.* at system sizes  $L > L_c$ . Moreover, the crossover length scale  $L_c$  increases with the pinning strength  $\lambda$  so that the critical behavior of the toy model can be obtained asymptotically at large system sizes.

However, our toy model exhibits the critical behavior of Narayan *et al.* if the initial condition is flat,  $m_i = 0$  for all  $i$ . Whereas the  $(\pm)$ -threshold states of the toy model have well coordinates which differ in at most four locations, the flat and  $(+)$ -threshold configurations are substantially different, and the evolution in the rank representation is more complicated. Instead of a single trapezoidal bump growing by avalanches, we have separated regions of activity which grow and merge. We will report elsewhere [15] on a more detailed investigation of this behavior.

## ACKNOWLEDGMENTS

DK and MM thank F. Rezakhanlou for stimulating discussions. MM acknowledges discussions with H.J. Jensen and M.M. Terzi. He thanks the Berkeley Math department for their kind hospitality during his sabbatical stay. This work was supported in part by NSF grant DMS-1106526 and Boğaziçi University grant 12B03P4.

- 
- [1] D. S. Fisher, Phys. Rev. Lett **50**, 1486 (1983)
  - [2] D. S. Fisher, Phys. Rev. B **31**, 1396 (1985)
  - [3] S. N. Coppersmith, Phys. Rev. Lett. **65**, 1044 (1990)
  - [4] S. N. Coppersmith and A. J. Millis, Phys. Rev. B **44**, 7799 (1991)
  - [5] O. Narayan and D. S. Fisher, Phys. Rev. B **46**, 11520 (1992)
  - [6] P. Le Doussal, K. J. Wiese, and P. Chauve, Phys. Rev. B **66**, 174201 (2002)
  - [7] D. Ertas and M. Kardar, Phys. Rev. B **53**, 3520 (1996)
  - [8] P. B. Littlewood, Phys. Rev. B **33**, 6694 (1986)
  - [9] A. Erzan, E. Veermans, R. Heijungs, and L. Pietronero, Phys. Rev. B **41**, 11522 (1990)
  - [10] C. R. Myers and J. P. Sethna, Phys. Rev. B **47**, 11171 (1993)
  - [11] A. Rosso and W. Krauth, Phys. Rev. E **65**, 025101 (2002)
  - [12] H. J. Jensen, J. Phys. A **28**, 1861 (1995)
  - [13] A. A. Middleton and D. S. Fisher, Phys. Rev. B **47**, 3530 (1993)
  - [14] O. Narayan and A. A. Middleton, Phys. Rev. B **49**, 244 (1994)
  - [15] D. C. Kaspar and M. Mungan, in preparation
  - [16] C. Tang, K. Wiesenfeld, P. Bak, S. Coppersmith, and P. Littlewood, Phys. Rev. Lett. **58**, 1161 (1987)
  - [17] F. Redig, in *Mathematical Statistical Physics, Volume LXXXIII: Lecture Notes of the Les Houches Summer School 2005*, edited by A. Bovier, F. Dunlop, A. V. Enten, F. D. Hollander, and J. Dalibard (Elsevier Science, 2006)
  - [18] D. L. Turcotte, Rep.Progr. Phys. **62**, 1377 (1999)
  - [19] Y.-C. Zhang, Phys. Rev. Lett. **63**, 470 (1989)
  - [20] The same is in fact true for the untruncated model with the corresponding adaptation of the ZFA [15].
  - [21] With probability  $1 - L^{-1}$  [15]
  - [22] J. T. Chayes, L. Chayes, D. S. Fisher, and T. Spencer, Phys. Rev. Lett. **57**, 2999 (1986)
  - [23] Consisting of functions which are right-continuous with left-limits
  - [24] Here and in the the following addition and subtraction of indices are mod  $L$ .
  - [25] E. V. Ivashkevich, D. V. Ktitarov, and V. B. Priezhev, Physica A **209**, 347 (1994)
  - [26] N. Glick, AMM **85**, 2 (1978)
  - [27] B. C. Arnold, N. Balakrishnan, and H. N. Nagaraja, *Records* (Wiley, 1998)
  - [28] The system size  $L$  bounds  $j_L + j_R$ .
  - [29] D. Dhar, Phys. Rev. Lett **64**, 1613 (1990)
  - [30] P. Ruelle and S. Sen, J. Phys. A **25**, L1257 (1992)
  - [31] G. Pruessner, *Self-Organized Criticality - Theory, Models and Characterisation* (Cambridge, 2012)